JOURNAL OF PHYSICAL ORGANIC CHEMISTRY
J. Phys. Org. Chem. 2000; **13**: 167–175

Ab initio study toward designing transition-state analogues which elicit proteolytic catalytic antibodies

Kazuko Shimazaki[1]*, Hiroyuki Kakinuma[1], Kyoko Takahashi[1], Shigeo Niihata[1], Naoko Takahashi[1], Hajime Matsushita[1], Yoshisuke Nishi[1] and Kazuhisa Sakakibara[2]

[1]Laboratory of Life Science and Biomolecular Engineering, Japan Tobacco Inc., Yokohama 227-8512, Japan
[2]Faculty of Engineering, Department of Synthetic Chemistry, Yokohama National University, Yokohama 240-8501, Japan

Received 4 July 1999; revised 20 August 1999; accepted 9 September 1999

ABSTRACT: New haptens useful for eliciting proteolytic antibodies are proposed. Transition state conformations of the amide and ester bond cleavages of simple quantum models were obtained by HF/6–31G* *ab initio* calculations. The results suggested that in our model of the transition state, forming the tetrahedral structure at the carbonyl carbon in a nucleophilic addition step is sufficient for ester bond cleavage, while formation of both the tetrahedral structure and the appropriate orientation of the lone-pair electrons on the nitrogen for the proton addition is necessary for amide bond cleavage. The key feature for designing good and/or potent haptens deduced from the transition state model could therefore be that both the tetrahedral conformation at the carbonyl carbon and proper orientation of lone pairs are simultaneously and appropriately reproduced in the haptens. Based on calculations, we designed potentially appropriate new haptens with the phosphonamidate functional group for eliciting proteolytic antibodies. Copyright © 2000 John Wiley & Sons, Ltd.

KEYWORDS: catalytic antibody; proteolytic activity; transition-state analogue; phosphonamidate

INTRODUCTION

It is our strong aim to elicit catalytic antibodies that can cleave the amide bond, as a major application of catalytic antibodies will be in the field of therapeutic use in medicine. In this regard, generation of the catalytic antibodies expressing proteolytic activity is of special value.

A large number of catalytic antibodies have been elicited by haptens designed as transition-state analogues.[1–7] The strategy is based on transition-state theory, which proposes that an antibody specific against a transition-state analogue will be more specific for the substrate at the transition state rather than at the corresponding ground state, and the differential binding energy for the transition state vs the ground-state is reflected as a rate acceleration.[8]

In previous studies, the use of haptens having a phosphonate moiety as a functional group led to the selection of catalytic antibodies with esterolytic but not proteolytic activity.[1–5] Since these haptens were considered to be a transition-state analogue for both ester and amide hydrolyses in which the tetrahedral conformation of the carbonyl carbon and the anionic characteristics of the carbonyl oxygens in the transition states were reproduced, there could be an essential difference in the mechanism between the proteolytic and esterolytic processes, or in the efficacy of eliciting proteolytic and esterolytic activity. In any case, however, no rules have been proposed for an appropriate measure for designing haptens, whether or not such haptens could be used for eliciting antibodies that cleave the amide bond instead of the ester bond.

In order to design haptens for proteolytic antibodies, more information about the mechanism of the cleavages is of particular importance. Estimations of the transition states of amide and ester bond cleavages and their comparison are urgently required.

For the chemical reaction, Pranata,[9] O'Brien and Pranata[10] and Hori and co-workers[11,12] proposed a mechanism for the base-promoted hydrolyses of the amide and ester bonds (Scheme 1). In both bond cleavages, the reactions proceed by a similar mechanism. The initial process is the nucleophilic addition of hydroxide to form a tetrahedral intermediate (step 1). The tetrahedral intermediate then undergoes conformational changes before the elimination reaction step (step 2). The difference between the ester and amide bond cleavages in the chemical reaction is that the highest energy point in the ester hydrolysis occurs during the nucleophilic addition step, whereas in the amide hydrolysis it occurs during the elimination step.[10,12–14]

**Correspondence to:* K. Shimazaki, Tobacco Science Research Laboratory, Japan Tobacco Inc., 6-2 Umegaoka, Aoba-ku, Yokohama, Kanagawa 227-8512, Japan.
E-mail: kazuko.shimazaki@ims.jti.co.jp
Contract/grant sponsor: NEDO (New Energy and Industrial Technology Development Organization).

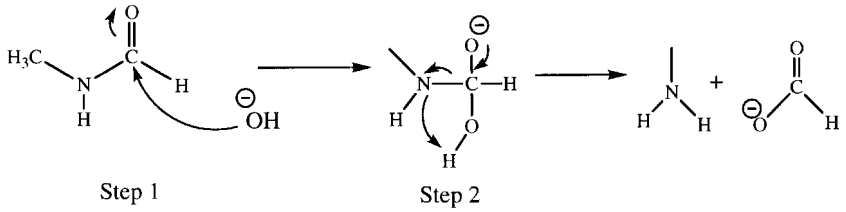

Scheme 1. Mechanism of base-promoted hydrolysis of the proposed amide.[10]

In enzymatic reactions, serine proteases are the most studied among the proteases, both experimentally and theoretically.[15–23] X-ray analysis revealed that the triad structure of the active site, e.g. serine 195, histidine 57 and aspartic acid 109 in chymotrypsin, plays an important role in catalysis.[24] Based on semi-empirical molecular orbital calculations, Kollman and co-workers proposed a mechanism for amide and ester bond cleavage (Scheme 2) at the active site of the enzyme.[21–23] The mechanism consists in two steps, formation of the tetrahedral intermediate of the substrate (step 1) and elimination after the conformational change has occurred by bond rotation around the C—N bond (steps 2 and 3). Comparison of chemical and enzymatic reactions of amide hydrolysis demonstrated that the proton in the elimination step in the chemical reaction (Scheme 1, step 2) corresponds to concerted release of a proton from the oxygen of the serine by the cooperative work of the acid catalyzed by His 57 in the enzymatic hydrolysis (Scheme 2). They found that the formation of the tetrahedral intermediate (Scheme 2, step 1) is a rate-determining step and protonation to the nitrogen (Scheme 2, step 3) resulting in the cleavage of the amide bond is a subsequent rate-determining step. Krug *et al.* proposed that the enzymatic action of serine protease could be the result of N^{τ} of the imidazolyl of His, providing the concerted general base and acid catalysis.[13]

These studies suggested that reproducing the tetrahedral conformation of the carbonylcarbon by the phosphonate moiety in the haptens is not sufficient, because it only mimics the intermediate in the nucleophilic attack step, as is shown in the chemical reaction (Scheme 1, step 1) or in the enzymatic reaction (Scheme 2, step 1).

The key feature for designing a hapten for proteolytic activity could therefore be to reproduce the transition-state conformation during the steps of both the nucleophilic addition and elimination in one hapten simultaneously, as only one-step selection using a single hapten is allowed from a wide variety of antibody repertoires.

For this purpose, we adopted a ‘one-step model’ for

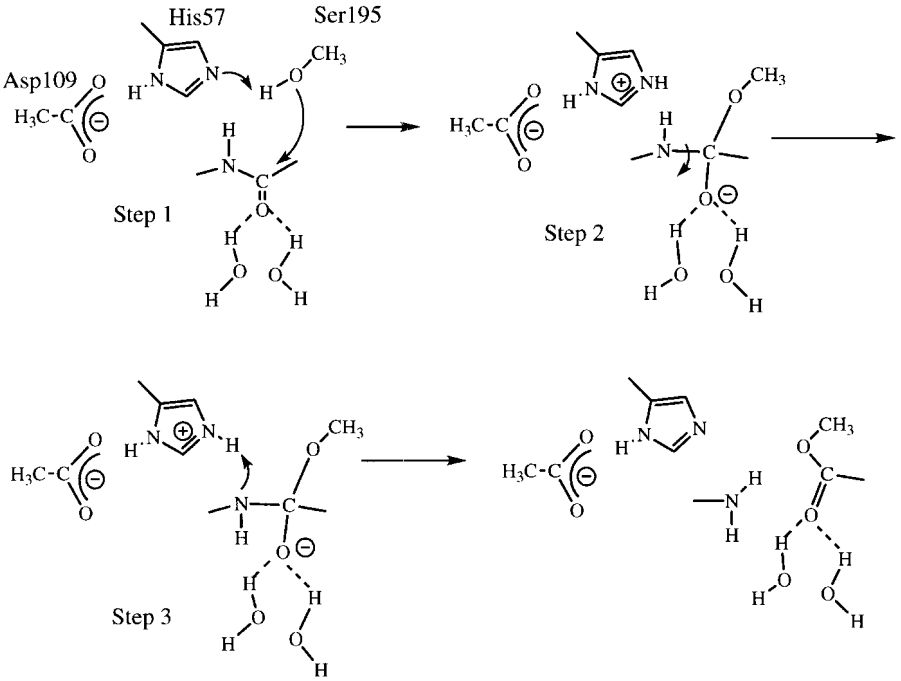

Scheme 2. Mechanism of amide bond hydrolysis by serine protease.[21–23] For convenience, we named our hydrolysis mechanism the ‘one-step model’ and the general hydrolysis mechanism described above as the ‘two-step model.’

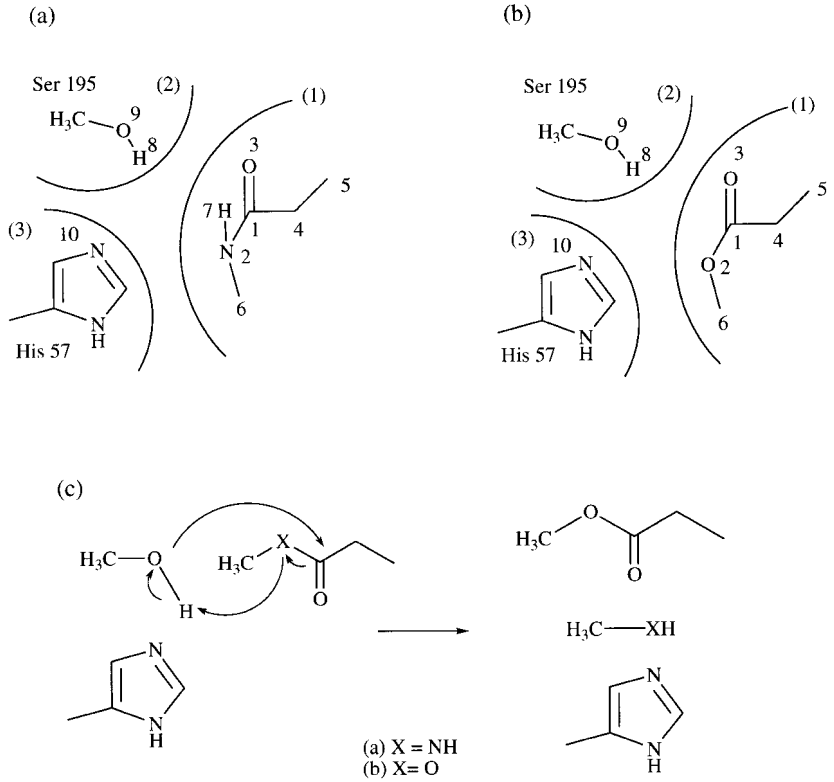

Figure 1. Structures of the modeled substrates and interacting amino acids in the enzyme active site for (a) amide and (b) ester, and (c) the adopted one-step mechanism. Models (a) and (b) were used for transition-state calculation of the one-step mechanism (c). The substrates of amide and ester were simplified as *N*-methylpropionamide [(1) in (a)] and methylpropionate [(1) in (b)], respectively. Serine 195 and histidine 57 were replaced by methanol (2) and 5-methylimidazole (3), respectively

amide bond cleavage in the catalytic triad in serine proteases.[25] Aided by computational chemistry, we planned to design an appropriate hapten for eliciting proteolytic antibodies. First, we examined the transition-state structure and electronic properties of the process of amide bond cleavage using our quantum models elucidate the exact process of ester and amide hydrolysis in the model of the enzymatic active site mimicking the serine protease catalytic site. We then designed several transition-state analogue candidates appropriate for use as a hapten eliciting proteolytic activity. Among the antibodies elicited against such a hapten, we can expect to find good antibodies (catalytic antibodies) having a moiety composed of the catalytic-site-like triad in the binding site for functioning as protease mimics.

EXPERIMENTAL

Conformational analyses of transition states

To design a hapten for reproducing the transition-state structures in both the nucleophilic addition and elimination steps, we assumed a mechanism of the hydrolyses of the amide or ester bond in such a way that the nucleophilic addition to the carbonyl carbon and the elimination of the leaving group occur simultaneously. We tried to find the transition states of amide and ester bonds based on the above 'one-step model' in the modeled catalytic triad in serine protease. The relative coordinates of Ser 195 and His 57 were derived from the x-ray structure [α-chymotrypsin (EC 3.4.21.1, 1cho.pdb in the Protein Data Bank)][24] In our model, Ser 195 and His 57 residues and the substrate were simplified and replaced by methanol, 5-methylimidazole and *N*-methylpropionamide for the amide model [Fig. 1(a)] and by methyl propionate for the ester model [Fig. 1(b)]. As the initial geometry, we adopted the amide substrate with an '*N-syn* conformation' in which the N2—H7 and C1—O3 bonds were eclipsed with respect to the C1—N2 bond [Fig. 1(a)]. For comparison, we also adopted an ester model with the same conformation around the C1—O2 bond rotation of the substrate as the initial geometry [Fig. 1(b)].

Full geometry optimization of the transition-state calculations including vibrational analyses were performed at the HF/6–31G* level. The energy was recalculated with MP2/6–31G* by using the optimized geometries at the HF/6–31G* level. All *ab initio* calculations were performed using Gaussian 94 (Revision D.4)[26] on DEC Alpha workstations.

Table 1. Structural parameters of the transition states

Parameter	Amide model		Ester model	
Distances (Å):				
	C1—N2	1.502	C1—O2	1.622
	C1—O9	2.247	C1—O9	1.916
	N2—H8	1.036	O2—H8	1.051
	O9—H8	1.721	O9—H8	1.391
	N10—H8	2.492	N10—H8	3.700
Angles (°):				
	∠O3—C1—N2	116.1	∠O3—C1—O2	112.9
	∠O3—C1—O9	112.5	∠O3—C1—O9	112.4
	∠O3—C1—C4	127.2	∠O3—C1—C4	130.2
	∠H7—N2—H8	106.9		
	∠H7—N2—C6	110.8		
	∠H8—N2—C6	115.8		
	∠N2—C1—C4	115.1	∠O2—C1—C4	110.6
Torsion angles (°):				
	∠C4—C1—N2—C6	54.5	∠C4—C1—O2—C6	22.9
Bond population:				
	C1—N2	0.3267	C1—O2	0.1399
	C1—O9	0.1237	C1—O9	0.1862
Imaginary frequency (cm^{-1})		195.66i		873.94i

[a] The numbering system is shown in Fig. 1.

Conformational analyses of the reported haptens

Phenyl ethylphosphonate (**1**) and *p*-nitrophenyl ethylphosphonate (**2**) were adopted as the models of the haptens which could elicit esterolytic antibodies.[3,4] *N*-(*p*-Nitrophenyl) benzylphosphonamidate (**3**) was adopted as the hapten for the hydrolysis of anilide.[6] The possible stable conformers were searched for and their geometries were optimized by the MP2/6–31G* calculations.

To evaluate the direction of the lone-pair orbital, the negative electrostatic potential surfaces (N-EPS) were calculated both for the optimized transition-state structures of the substrates and for those of the haptens.

RESULTS

Transition-state model analysis

Structural parameters of the transition-state models of the substrates. Structural parameters of the transition-state models are listed in Table 1. The vibrational modes for the single imaginary frequencies inherent to the amide and ester transition states are indicated by the arrows [Fig. 2(a) and (b)].

In the amide model, the transition state was found with a single imaginary frequency (195.66 i cm^{-1}) in our 'one-step model.' The vibrational mode showed that the OH proton of Ser 195 (H8) leaves the Ser 195 oxygen (O9) while the carbonyl carbon (C1) of the substrate approaches the Ser 195 oxygen (O9). Then the amide bond (C1—N2) is lengthened to take an appropriate orientation for the proton (H8) attack on the lone pair of the nitrogen atom (N2). The carbonyl carbon (C1) loses its planar structure and tends to take a tetrahedral conformation; the amide nitrogen (N2) becomes pyramidalized. IRC (intrinsic reaction coordinate) calculation confirmed that the structure obtained corresponds to the transition state for the C—N bond cleavage.

In the ester model, the transition state was found with the wavenumber for the imaginary frequency of 873.94 i cm^{-1}. The vibrational mode of this imaginary frequency shows that a similar movement found in the case of the amide model was observed with respect to the OH proton (H8) leaving Ser 195 and breaking the ester C1—O2 bond. By IRC calculation, the transition state was shown to be valid for C—O bond cleavage.

The geometries of the transition states and the overlap populations of the relevant bonds in both steps of bond cleavage and bond formation are also summarized in Table 1. In the transition state of the amide model, the bond population for breaking the amide bond (C1—N2) (0.3267) was larger than that forming the carbonyl carbon—oxygen bond of Ser 195 (C1—O9) (0.1237). The distance between C1 and N2 (1.502 Å) was shorter than that between C1 and O9 (2.247 Å). Comparing the transition-state structure with that of the ground state, the C1—N2 bond was lengthened and the C1—O9 bond was shortened. In the transition state of the ester model, however, the bond population of the newly forming C1—O9 bond (0.1862) was larger than that of the breaking ester C1—O2 bond (0.1399). The length of the C1—O2 bond (1.622 Å) was shorter than that of the C1—O9 bond (1.916 Å).

Conformational and electronic properties of the transition-state models of the substrates. The directions of the lone-pair electrons evaluated by

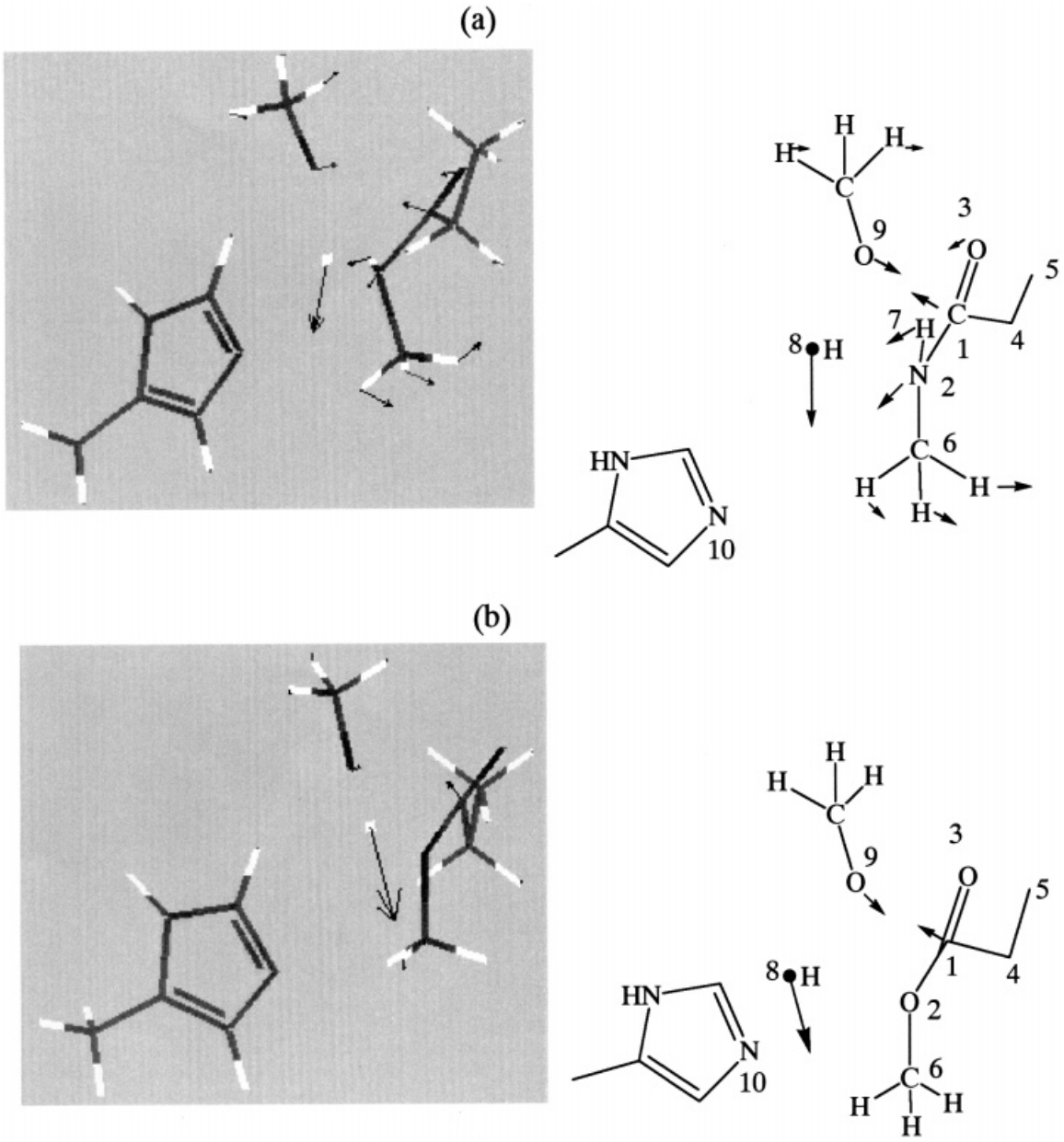

Figure 2. Transition-state structures of (a) amide and (b) ester bond cleavage obtained by HF/6–31G* calculations. The arrows indicate the vibrational mode of the single imaginary frequency in the transition state structures of amide and ester

depicting the negative electrostatic potential surface (N-EPS) are shown in Plate 1. Judging from the N-EPS in the amide model, the lone pair on the amide nitrogen (N2) atom was oriented towards the entering proton (H8). In contrast, the N-EPS in the ester model was spread half-spherically around the alkoxy oxygen O2. These models demonstrated that the lone-pair electrons in the amide model are more directionally oriented than in the ester model.

Hapten analysis

First, the optimized structures together with N-EPS of the most stable conformers of the reported haptens were obtained (Plate 2). All stable conformers of **1, 2** and **3** held the tetrahedral conformation around the phosphonyl moiety. In the transition-state analogues of phosphonate (**1** and **2**), two oxygen atoms (O3 and O3′) in the O—P—O moiety (each held *pro-S* and *pro-R* positions) were set to correspond to the carbonyl oxygen and the nucleophilic oxygen in the transition-state model. The *O*-aryl moiety held an *anti* conformation with respect to the P1—C4 bond. The N-EPS on the aryl oxygen (O2) was extended to the opposite side to the *pro-R* phosphonyl oxygen (O3). In contrast, in the transition-state analogue of phosphonamidate (**3**), the *N*-aryl moiety held a *gauche* conformation with respect to the P1—C4 bond, and the

Table 2. Values of ELp[a]

Transition-state model:	
Amide	2.43
Ester	2.39
Existing haptens:	
1	0
2	0
3	1.20
Designed haptens:	
4	0.34
5	1.55
6	0
7	1.94
8	2.23

[a] The ELp is defined according to the following equations:

$$fr^{(N)} = 2C^2\text{r(lone-pair-orbital)} \quad (1)$$

$$\text{Lp} = \sum_{\mu=1}^{M} fr^{(N)}\mu/|E(\text{lone-pair orbital})\mu| \times \text{Pop}\mu \quad (2)$$

$$\text{ELp} = \sum_{\mu=1}^{M} fr^{(N)}\mu/|E(\text{lone-pair orbital})\mu| \times \text{Pop}\mu \times A \quad (3)$$

where $fr^{(N)}$ is the electron density of oxygen or nitrogen in the lone-pair orbital, Cr is the coefficient in the lone-pair orbital, $|E$(lone-pair orbital)$|$ is the absolute value of the lone-pair orbital energy (hartree) and Pop is the population of the local minimum at 25 °C; μ is the number of local minima. [ELp] involves contribution factor A with regard to the orientation of the lone pair on oxygen or nitrogen. In this case, the contribution factor A was defined as follows: $A = 1$ if the lone pair takes the antiperiplanar conformation with respect to the P1—C4 bond; in other cases, $A = 0$. The lone-pair orbital that has large coefficients of $2p_z$ or $3p_z$ on the nitrogen or oxygen atoms (and that has an antiperiplanar orientation with respect to the P1—C4 bond) was deduced using Boys' method.[33]

N-EPS on the aryl nitrogen (N2) was extended antiperiplanar with respect to the P1—C4 bond. The N-EPS of the phosphonamidate **3** showed a more similar orientation of the lone-pair electrons to the transition state model of the amide than that of the phosphonates (**1** and **2**).

New haptens designed with the lone pair in antiperiplanar orientation with respect to the P—C bond based on the phosphonamidate (**3**) are demonstrated in Plates 3 and 4. To compare alkyl phosphonamidate and aryl phosphonamidate further the conformation and N-EPS of *N*-methyl phosphonamidate (**4**) and *N*-phenyl benzylphosphonamidate (**5**) are shown. The nitrogen (N2) of the most stable conformer of **4** has the sp^3 conformation, and the lone-pair orientation on nitrogen was synperiplanar with respect to the P1—C4 bond. Three stable conformers of **5** with the conformational difference at the benzyl moiety (Nos 1, 2 and 3 in Plate 3) are shown. These conformers took an sp^3-like conformation at the nitrogen (N2) and did not form a planar conformation around the P—N—aryl moiety. The lone-pair on nitrogen (N2) was oriented antiperiplanar with respect to the P1—C4 bond in all conformers.

Based on the above information, new haptens with an *N*-alkyl phosphonamidate moiety were further designed. The conformation and N-EPS at the global minima of the new haptens are depicted in Plate 4. To constrain the orientation of the lone pair to the antiperiplanar direction, the six-membered cyclic compound **6** was further designed. The chair form was the dominant conformation, and its N-EPS at the nitrogen (N2) was extended to a synclinical orientation with respect to the P1—C4 bond (Plate 4). Fluorine atoms were then introduced to the carbon adjacent to the phosphonyl oxygens (**7** and **8**). We expected that the orientation of the lone-pair on the nitrogen (N2) might change from synperiplanar to antiperiplanar by the diplole–dipole and/or charge–dipole interactions between the phosphonamidate moiety and the fluorine atoms. Actually, *ab initio* calculations indicated that the dominant conformation of **7** and **8** took an expected antiperiplanar conformation of the lone pair with respect to the P1—C4 bond.

To evaluate the newly designed haptens parametrically, we introduced the 'effective lone-pair parameter' (ELp) as a new index whose value shows the degree of proper orientation of the lone pair for the elimination step of the amide bond cleavage. The equation is given in Table 2. The ELp values for the transition states of the modeled substrates and the reported haptens are listed in Table 2. The ELp values for the transition-state substrates of the amide and ester were 2.43 and 2.39, those for the ary phosphonamidate haptens (**3** and **5**) were 1.20 and 1.55 and those for haptens with a phosphonate moiety (**1** and **2**) were zero (Table 2). The values for **7** and **8** (1.94 and 2.23) were close to those of the transition states of the model substrates.

DISCUSSION

We set out to design a hapten useful for obtaining catalytic antibodies that catalyze amide bond cleavages. Amide bond cleavage in both chemical and enzymatic reaction is generally considered to proceed in two steps, nucleophilic addition and elimination.[10–23] In the serine protease-catalyzed cleavage of amides, however, Komiyama and Bender proposed an S_N2-like one-step reaction.[25] In this model, the reaction proceeds in such a way that the nucleophilic addition to the carbonyl carbon and elimination of the leaving group occur simultaneously.

From the standpoint of hapten design, an inevitable desire is to reproduce a transition-state-like structure in a single hapten. To satisfy this requirement, we must follow the one-step model, such as that proposed by Komiyama and Bender for amide bond cleavage reactions, rather than the generally accepted two-step model.[15–23]

If we can find a candidate for a transition state that fits the bond cleavage reaction following the one-step model, it will then be plausible to design a single hapten that elicits antibodies catalyzing the amide bond cleavage reaction. Aided by computational chemistry, we propose

here a possible one-step model for amide bond cleavage and find that it gives an insight into the design of a potent hapten capable of eliciting amide bond-cleaving activity.

Our one-step model of the amide and ester bond cleavage consists of Ser, His and the substrate. As the initial geometry of the amide substrate, we adopted the *N-syn* conformation. In that geometry, the C═O bond and N—CH_3 bond were arranged in a staggered conformation, which appeared in the elimination step of the two-step model.[21,22,27] In fact, we could not reach the transition-state conformation where the C═O bond and N—CH_3 bond were in an eclipsed form. We also tried to optimize the transition state of the ester bond cleavage with the conformation in which the C═O bond and O—CH_3 bond were set in an eclipsed conformation as the initial conformation in our one-step model, but we could not do so. Therefore, the same conformation as the amide substrate, in which the C═O bond and O—CH_3 bond were arranged in staggered conformation, was adopted as the initial geometry of the ester substrate. The result was a contrast to that obtained in the other studies following the one-step model.[20] Their ester substrate took on an eclipsed conformation around the C═O and O—CH_3 bonds. The difference in the initial conformation between those studies and our model may be due to the addition of one free water molecule to the model in their studies. This molecule may act as a catalyst, whereas in our model the OH proton of Ser was directly attracted by the amide nitrogen.

In our model of ester bond cleavage, the bond population of the cleaving bond (C1—O2) is smaller than that of the forming bond (C1—O9), and the vibrational mode at the transition state indicates that the H8 proton is attracted to the lone pair on the alkoxy oxygen (O2), so the elimination step occurs spontaneously by the movement of the H8 proton. These results suggest that the change of the carbonyl carbon (C1) from a planar to a tetrahedral conformation is sufficient for the ester bond cleavage. In contrast, in the amide bond cleavage, the bond population of the cleaving bond (C1—N2) is larger than that of the forming bond (C1—O9) and its vibrational mode at the transition state shows that the planarity of the carbonyl carbon (C1) is decreasing and that pyramidalization at the nitrogen atom (N2) from sp^2 to sp^3 is proceeding.

The studies on a two-step model proposed that the difference between amide bond and ester bond cleavage resides in the elimination step. In amide bond cleavage, the lone pair must be arranged in a proper position to accept the proton from hydroxide, whereas in the ester bond cleavage, cleavage occurs spontaneously when the carbonyl carbon is changed from sp^2 to sp^3 in the nucleophilic step.[10,12–14] In our one-step model, the results are fairly consistent with those described above. The important process in the amide bond cleavage is the protonation to the amide nitrogen upon losing planarity at the carbonyl carbon and pyramidalizing the amide nitrogen, whereas in the ester bond cleavage, it was not the protonation but the sp^3 conformation at the carbonyl carbon that is important.

As the transition state could be obtained, the electronic properties of amide and ester substrates at the transition state could be further calculated and evaluated. In this analysis, we chose the N-EPS. Judging from the distribution of the N-EPS, the OH proton (H8) can be abstracted to the lone-pair on the ester oxygen (O2) from a wide direction. In comparison, the entering direction for the OH proton (H8) is very limited in the case of the amide nitrogen (N2), because the lone pair on the amide nitrogen (N2) appears in the proper direction by losing the planarity of the carbonyl carbon (C1) and amide nitrogen (N2). From these findings, we speculate that protonation to the lone pair on the amide nitrogen (N2) is more difficult than to that on the ester oxygen (O2).

We further examined N-EPS of the reported phosphonate-based haptens (**1** and **2**) that could elicit esterolytic antibodies.[3–5] The results revealed that the tetrahedral conformations were well reproduced around the phosphonate moiety and large N-EPS around the phosphonyl oxygens (O3 and O3′) were observed. It is considered that such a large N-EPS plays an important role in stabilizing the tetrahedral intermediate of ester in the catalytic pocket.[28,29] For stabilization, the hydrogen bonding and the electrostatic interactions play a part, and the x-ray analyses suggested that these interactions between the phosphonyl oxygens (O3 and O3′) of haptens and the catalytic binding site were formed in the esterolytic antibodies.[30] The most likely mechanism for the esterolytic antibodies elicited against **1** and **2** involves direct hydroxide attack from free water rather than a side-chain of the amino acid on the scissile carbonyl carbon of ester, facilitated by the specific stabilizing interactions with the oxyanionic transition state species.[30]

It is noteworthy that each lone pair of the alkoxy oxygen (O2) in **1** and **2** was not oriented to the proton entering side, which should be required for amide bond cleavage, because the repulsion of the lone pair between the alkoxy oxygen (O2) and the phosphonyl oxygens (O3 and O3′) prevented the lone pair from locating the proton entering side. This may be the reason why these phosphonate-based haptens could not elicit proteolytic activity. Again, these haptens could mimic only the transition state for the nucleophilic step and not the step of elimination in the amide bond cleavage.[3–5] In other words, the hapten that can elicit the proteolytic antibody must mimic the transition state of both nucleophilc addition to the carbonyl carbon and protonation to the amide nitrogen. A plausible mechanism for such proteolytic antibodies must involve nucleophilic attack from the side-chains of the amino acid in the catalytic active site and protonation to the amide nitrogen following a concerted fashion, facilitated by the more appropriate stabilizing interactions between surrounded amino acid side-chains and the transition-state species

and by the proton in the appropriate position. For eliciting the esterolytic antibody, it is sufficient to reproduce the transition state of the nucleophilic addition to the carbonyl carbon by the phosphonate moiety. Hence, the hapten appropriate for esterolytic antibody just requires holding the tetrahedral conformation with a large N-EPS.

Our one-step model has a good reason for explaining why hapten **3** could elicit antibodies with an amide hydrolysis-like reaction, anilide hydrolysis. In haptens **3** and **5**, the orientation of the lone pair of the nitrogen is closer to the proton-entering side at the amide nitrogen (N2). In spite of the adjacent *N*-aryl group, the P—N—aryl moiety does not form a planar conformation and the nitrogen (N2) takes an sp^3 like conformation. As a result, **3** and **5** can maintain a better orientation of the lone pair of nitrogen for eliciting anilide hydrolysis than the other haptens. In the anilide hydrolytic antibody elicited against **3**, a histidine attacks the scissile carbonyl carbon as a nucleophile. As a result, a covalent acyl intermediate was formed.[7,30,31] Although the mechanism of the protonation to the anilide nitrogen is not clear, the appropriate orientation of the lone pair on the anilide nitrogen seems to play an important role in the protonation.

From the above, we designed some haptens based on phosphonamidates, such as **4**–**8**. To evaluate the potency of these designed haptens appropriate for amide cleavage, we introduced a new parameter (ELp), which includes both the electronic properties and the orientation of the lone pair. In a comparison of ELp between esterolytic (**1** and **2**) and anilide hydrolytic haptens (**3**), the difference in eliciting potency between esterolytic and proteolytic catalytic antibody can be represented by the ELp values. To increase the ELp score, we tried to design new haptens. First, a simplified model of phosphonamidate (**4**) was introduced. The dominant conformer of **4** showed that the repulsion of the negative charge between two phosphonyl oxygens (O3 and O3′) and lone pair on nitrogen (N2) caused a synperiplanar orientation of the lone pair on nitrogen (N2) with respect to the P1—C4 bond. This conformation was similar to those of the reported haptens (**1** and **2**) that could only elicit estrolytic antibodies. As a result, the ELp score of **4** was zero, the same as for **1** and **2**. We then introduced fluorine atoms to the carbon adjacent to phosphonyl oxygens (**7** and **8**). The orientation of the lone pair on nitrogen (N2) changed dramatically from synperiplanar to antiperiplanar with respect to the P1—C4 bond. These haptens now have larger ELp scores (1.94 and 2.23) than those of *N*-aryl phosphonamidates **3** and **5** (1.20 and 1.55). Judging from the ELp scores, **7** and **8** could be more appropriate candidates than **3** and **5** to elicit proteolytic active antibodies. Compared with **7**, the lone-pair orientation in **8** is better constrained to the proper position by the cyclic conformation, and it is reflected by the larger ELp of **8** than **7**. The dramatic change in the orientation of the lone pair on the nitrogen (N2) from synperiplanar to antiperiplanar with respect to the P1—C4 bond can be induced by the electronic interactions due to the dipole–dipole and/or charge–dipole among the C—F, P—O and P—N bonds and lone-pair electrons. In **7** and **8**, an orbital interaction between the lone-pair orbital on nitrogen (N2) and the antibonding orbital of the P1—C4 bond is possible when they assume an antiperiplanar conformation. This orbital interaction leads to bond length changes of the relevant bonds. The P1—N2 bond shortens whereas the P1—C4 bond lengthens (*trans* lone-pair effect).[32] This change can be easily recognized by comparing the bond lengths of **8** with those of **6** (no *trans* lone-pair effect). The P1—N2 bond lengths of **8** and **6** are 1.760 and 1.736 Å and the P1—C4 bond lengths are 1.842 and 1.872 Å, respectively.

Finally, to our knowledge, this is the first study on the design of new haptens for amide bond cleavages using computational chemistry for evaluating the reaction, the structure and the electrostatic properties of the transition state and transition-state analogues. A study to determine whether these new haptens will really be potent in eliciting catalytic proteolytic antibodies is under way.

Acknowledgements

This work was supported in part by NEDO (New Energy and Industrial Technology Development Organization, Japan) as an R&D Project of the Industrial Science and Technology Frontier Program.

REFERENCES

1. Pollack SJ, Jacobs JW, Schultz PG. *Science* 1986; **234**: 1570–1573.
2. Tramantano A, Janda KD, Lerner RA. *Science* 1986; **234**: 1566–1570.
3. Zhou G-W, Guo J, Huang W, Fletterick RJ, Scanlan TS. *Science* 1994; **265**: 1059–1064.
4. Tawfik DS, Zemel RR, Arad-Yellin R, Green BS, Eshhar Z. *Biochemistry* 1990; **29**: 9916–9921.
5. Charbonnier J-B, Carpenter E, Gigant B, G-Pimpaneau B, Eshhar Z, Green BS, Knossow M. *Proc. Natl. Acad. Sci. USA* 1995; **92**: 11721–11725.
6. Janda KD, Schloeder D, Benkovic SJ, Lerner RA. *Science* 1988; **241**: 1188–1191.
7. Stewart JD, Litta LJ, Benkovic SJ. *Acc. Chem. Res.* 1993; **26**: 396–404.
8. Jacobs JW. *Biotechnology* 1991; **9**: 258–262.
9. Pranata J. *J. Phys. Chem.* 1994; **98**: 1180–1184.
10. O'Brien JF, Pranata J. *J. Phys. Chem.* 1995; **99**: 12759–12763.
11. Hori K. *J. Chem. Soc., Perkin Trans.* 1992; **2**: 1629–1633.
12. Hori K, Kamimura A, Ando K, Mizumura M, Ihara Y. *Tetrahedron* 1997; **53**: 4317–4330.
13. Krug JP, Popelier PLA, Bader RFW. *J. Phys. Chem.* 1992; **96**: 7604–7616.
14. Teraishi K, Saito M, Fujii I, Nakamura H. *Tetrahedron Lett.* 1992; **33**: 7153–7156.
15. Tapia O, Paulino M, Stamato FMLG. *Mol. Eng.* 1994; **3**: 377–414.
16. Kollman PA. *Curr. Opin. Struct. Biol.* 1992; **2**: 765–771.
17. Scheiner S, Lipscomb WN. *Proc. Natl. Acad. Sci. USA* 1976; **73**: 432–436.

18. Stamato FMLG, Longo E, Yoshioka LM, Ferreira RC. *J. Theor. Biol.* 1984; **107**: 329–338.
19. Stamato FMLG, Tapia O. *Int. J. Quantum. Chem.* 1988; **33**: 187–194.
20. Dive G, Dehareng D, Peeters D. *Int. J. Quantum. Chem.* 1996; **58**: 85–107.
21. Weiner SJ, Seibel GL, Kollman PA. *Proc. Natl. Acad. Sci. USA* 1986; **83**: 649–653.
22. Daggett V, Schröder S, Kollman P. *J. Am. Chem. Soc.* 1991; **113**: 8926–8935.
23. Stanton RV, Peräkylä M, Bakowles D, Kollman PA. *J. Am. Chem. Soc.* 1998; **120**: 3448–3457.
24. Fujinaga M, Sielecki AR, Read RJ, Ardelt W, Laskowski M, James MNG. *J. Mol. Biol.* 1987; **195**: 397–418.
25. Komiyama M, Bender ML. *Pro. Natl. Acad. Sci. USA*, 1979; **76**: 557–560.
26. Frisch MJ, Trucks GW, Schlegel HB, Gill PMW, Johnson BG, Robb MA, Cheeseman JR, Keith T, Petersson GA, Montgomery JA, Raghavachari K, Al-Laham MA, Zakrzewski VG, Ortiz JV, Foresman JB, Cioslowski J, Stefanov BB, Nanayakkara A, Challacombe M, Peng CY, Ayala PY, Chen W, Wong MW, Andres JL, Replogle ES, Gomperts R, Martin RL, Fox DJ, Binkley JS, Defrees DJ, Baker J, Stewart JP, Head-Gordon M, Gonzalez C, Pople JA. *Gaussian 94, Revision D.4*. Gaussian: Pittsburgh, PA, 1995.
27. Taira K, Gorenstein DG. *Bull. Chem. Soc. Jpn.* 1987; **60**: 3625–3632.
28. Radkiewicz JL, McAllister MA, Goldstein E, Houk KN. *J. Org. Chem.* 1998; **63**: 1419–1428.
29. Kakinuma H, Shimazaki K, Takahashi N, Takahashi K, Niihata S, Aoki Y, Hamada K, Matsushita H, Nishi Y. *Tetrahedron*, 1999; **55**: 2559–2572.
30. MacBeath G, Hilvert D. *Chem. Biol.* 1996; **3**: 433–445.
31. Siuzdak G, Krebs JF, Benkovic SJ, Dyson HJ. *J. Am. Chem. Soc.* 1994; **116**: 7937–7938.
32. Juaristi E, Cuevas G. *The Anomeric Effect*. CRC Press: Boca Raton, FL, 1995; 17–48.
33. Boys SF. *Rev. Mod. Phys.* 1960; **32**: 296–299.

